Adsorption 9: 153–164, 2003

The Adsorption of CHF_3 on NaY5.6 Zeolite and Microdynamic Behaviors in Small Pores

MITSUHIRO YOSHIKAWA MURATA AND MITSUMASA ISHIWATA*
Department of Physics, Saitama University, Saitama 338-8570, Japan
ishiwata@phy.saitama-u.ac.jp

TOSHIHISA YOSHIDA
Department of Science Education, Saitama University, Saitama 338-8570, Japan

Received July 24, 2002; Revised January 20, 2003; Accepted February 19, 2003

Abstract. Adsorption of CHF_3 on a NaY5.6 zeolite has been studied by the measurement of H and F NMR of the CHF_3 molecule, focusing in particular on the measurements of a chemical shift and a longitudinal relaxation time, together with the adsorption isotherm measurements. A coordination structure of the adsorbed CHF_3 is determined from the relationship between a chemical shift and an adsorption amount. Relaxation times of H and F were measured at respective two resonance frequencies for various adsorption amounts and temperatures. These relaxation data have been analyzed by use of the thermally activated diffusion model proposed by Torrey. From these analyses, various microdynamic variables such as a mean life time of the trapped state and a mean jump distance in the diffusion were determined as functions of an adsorption amount and temperature.

Keywords: adsorption, zeolite, trifluoromethane, H and F NMR, chemical shift, adsorption structure, translational diffusion, microdynamics in the pores

1. Introduction

Zeolites are porous crystals with a well-defined structure and a high specific surface area, widely used in industry as molecule sieves, as catalysis and ion exchangers. Equilibria and dynamics in physical adsorption on heterogeneous surfaces of zeolites and other microporous solids are actively being investigated from experimental and theoretical points of view (Rudzinski et al., 1997; Fraissard, 1997). The widespread application of microporous solids has also stimulated considerable interest in the study of diffusive transport of guest molecules in small pores (Kärger et al., 1992). Molecules adsorbed on a zeolite surface show either liquid-like or solid-like or in general an intermediate behavior. A study of microdynamic behavior of adsorbed molecules in such an intermediate state is not only of interest from a purely theoretical point of view, but it is also the key for a better understanding of industrial processes. From this angle on the problem, we have investigated adsorption of a simple polar hydrofluorocarbon molecule on a NaY5.6 zeolite ($SiO_2/Al_2O_3 = 5.6$).

Recently, we have reported the result for a $CHClF_2$ molecule adsorbed on the NaY zeolite (Yoshikawa et al., 2000), and we determined a coordinate structure of the adsorption molecule from a relationship between NMR chemical shift and an adsorption amount, and qualitatively explained experimental dependences of NMR relaxation times on an adsorption amount by using the intramolecular dipole interaction. The present paper deals with a more symmetric CHF_3 molecule adsorbed on the same zeolite. The CHF_3 molecule contains two magnetic nuclei ^1H and ^{19}F with high NMR

*To whom correspondence should be addressed.

Table 1. Impurity contents[a] of NaY5.6 zeolite

Cl	K_2O	CaO	TiO_2	Fe_2O_3
0.081 ± 0.009	0.018 ± 0.001	0.047 ± 0.002	0.066 ± 0.010	0.052 ± 0.001

[a]Weight percent.

sensitivities. Together with a volumetric measurement of adsorption amount and the chemical shift measurement similar to the case of the $CHClF_2$ molecule, we had done detailed relaxation measurements for the CHF_3 molecule; namely, temperature as well as adsorption amount dependences of a longitudinal relaxation time for both the H and F nuclei were observed. These relaxation measurements were done at two resonance frequencies around 90 MHz and 400 MHz. Marked frequency-dependences were obtained for the two nuclei at various loadings of the CHF_3 molecule.

Furthermore, analysis of X-ray emission spectra showed that our zeolite sample contained a paramagnetic impurity with an amount sufficient to control a relaxation time of the adsorbate. In this paper, thus, we will present results of quantitative analysis of the various relaxation data on the basis of translational diffusion of the adsorbed molecule and discuss microdynamic behavior in the porous zeolite. By adopting the thermally activated diffusion model proposed by Torrey (1953), various parameters such as a mean life time of the trapped state and a mean jump distance in the diffusion have been determined as functions of temperature and an adsorption amount.

2. Experimental

2.1. Zeolite Sample

The adsorbent we used was commercial synthetic NaY5.6 zeolite (Tosoh Co., Ltd., Japan). It was in a powdered form and contained no inert binder material. The adsorbate was commercial CHF_3 gas (Asahi Glass Co., Ltd., Japan). Its stated purity was better than 99%.

The zeolite in a sample tube was heated slowly to 673 K and evacuated under 10^{-5} Torr for 20 h. After these preparations, the CHF_3 gas was adsorbed on the zeolite at the constant temperature of 273 K or 293 K and adsorption amounts were measured on a volumetric apparatus. For NMR measurements, various amounts of the gas were adsorbed under the corresponding equilibrium pressure at 273 K and sealed into the NMR tube. The amount of adsorption was calibrated by use of an adsorption isotherm at 273 K.

2.2. Analysis of the Zeolite by an Electron Microscope

In order to determine a purity of the zeolite sample, especially to know the contents of paramagnetic impurities, the commercial NaY5.6 zeolite was analyzed by an electron microscope. The spectrometer used was JSM-6301F (JEOL Co., Ltd., Japan). X-ray emission spectra were observed under irradiation of the beam current of 0.01 μA from a probe with the diameter of 100 μm. Table 1 shows the impurity contents obtained. Thus, as only one type of paramagnetic impurity, the NaY zeolite contained a ferric iron of 364 ppm by weight, based on the dry weight of NaY5.6.

The electron microscope observation also showed that the zeolite used was small crystallites with a mean diameter of about 1 μm.

2.3. NMR Measurement

For the samples with various adsorption amounts of 4.5 to 55 molecule/cell, we measured NMR chemical shifts and longitudinal relaxation times T_1 of H and F nuclei in the CHF_3 molecule. In order to obtain data with high precision in the chemical shift measurement, a superconductive NMR spectrometer of AM400 (Bruker Co., Ltd., Japan) was used. Resonance frequencies were 400 and 376 MHz for H and F nuclei, respectively. The chemical shift measurements were done at a room temperature. Signal accumulations were done with 40 for H and 16 scans for F. Since the samples contained no NMR field-lock substance, we checked a standard resonance frequency at 0 ppm by using TMS and CCl_3F for H and F, respectively, before and after the measurement of each sample in order to make sure of no drift in the magnetic field.

For all the samples with various adsorption amounts, relaxation times T_1 of H and F were measured at 273 K by use of a spectrometer of FX90Q (JEOL Ltd., Co., Japan). Resonance frequencies of H and F are 89.5 and 84.3 MHz, respectively. The inversion recovery method was used in the measurement of T_1. T_1 values were determined by use of absorption peak areas. Signal accumulations were done with 16 to 160 scans for

H and 16 to 80 scans for F depending on an adsorption amount.

Choosing three adsorption amounts of 6.5, 15 and 55 molecule/cell as a representative one in low, middle and high loadings, we further measured the relationship between temperature and relaxation times T_1 for H and F nuclei of each sample by use of both the spectrometers AM400 and FX90Q; the temperature range was from 170 to 295 K. The sample temperature was regulated within 0.3 K using a conventional gas flow system. Temperature calibration was done by measurement of a splitting in H NMR signals of CH_3OH.

3. Magnetic Relaxation through Translational Diffusion in a NaY Zeolite

Nuclear magnetic relaxation of an organic small molecule, such as CHF_3, is usually due to the intramolecular or intermolecular dipole interaction in a non-magnetic medium. In a mobile state of the molecule, this mechanism gives rise to relatively slow relaxation with a time constant in the order of at least several tenth seconds or more depending on a molecule density and temperature (Ishiwata et al., 1995). As will be shown in chapter 4.3, however, typical longitudinal relaxation times T_1 of a proton in the CHF_3 molecule adsorbed on our sample are in the order of milliseconds. For an appropriate internuclear distance assumed, we couldn't obtain such a short T_1 value even from anisotropic rotational diffusion of the CHF_3 molecule (Werbelow et al., 1977). Furthermore, in F^{19} relaxation experiments we found little difference within experimental accuracy between T_1 values with or without proton decouplings. Thus, the intramolecular dipolar interaction does not have any substantial effect on the relaxation of the adsorbed CHF_3 molecule.

For the molecule adsorbed on a commercial synthetic faujasite, Resing and Thompson (1967) stressed the importance of paramagnetic Fe^{3+} impurities and explained the proton T_1 minimum of about 10 ms by using the dipolar interaction between electron and nuclear spins. Using various mixtures of cyclohexane and its deuterated one, Michel and Thöring (1971) also showed that the magnetic interaction with the Fe^{3+} impurities controlled proton T_1 in a commercial NaY zeolite. Furthermore, Pfeifer and his collaborators (1976a) have concluded that T_1 values of the adsorbent gas are completely determined by the electron-nuclear dipolar interaction when a NaY zeolite contains Fe^{3+} impurities more than 500 ppm by weight, and the relative contribution of the electron-nuclear dipolar interaction is estimated to run up to 70% of a T_1 value even for the Fe^{3+} content of about 50 ppm.

Our zeolite sample also contains the Fe^{3+} impurity of about 364 ppm by weight, as shown in the chapter 2. Therefore, we exclusively use the electron-nuclear dipolar interaction for the analysis of T_1 data. Since the Fe^{3+} ions are fixed to the zeolite skeleton structure (Derouane et al., 1974), the molecular motion which modulates the dipolar field, is translational diffusion of the molecules adsorbed on the zeolite.

Nuclear spin relaxation is essentially microscopic in character. Taking account of individual jump motion of the interacting spins, Torrey (1953) has developed a basic theory of the dipolar relaxation by atomic diffusion in polycrystalline solids. The specific dynamic model considered was one of the dipoles walking randomly through a lattice by jumps. The microscopic process of diffusion is characterized by a mean time τ_j between two jumps and a probability $P(\boldsymbol{r})$ that after one jump a spin is found at $\boldsymbol{r}$ relative to the previous position. In this report, we adopt the isotropic diffusion model, in which a uniform distribution of the paramagnetic impurities is assumed and model jumps of a diffusing molecule are allowed equivalently in random directions from the center of the paramagnetic impurity.

Assuming the mathematically simplest form for a Fourier transform of $P(\boldsymbol{r})$, moreover, Torrey (1953) proposed an interesting model for the *thermally activated diffusion*. In this model a closed form expression is obtained for T_1 under the following physical conditions. A spin can exist in one of two states: a trapped state or a thermally excited state in which the spin may move rapidly about in a random diffusive motion. It is assumed that the latter type of motion can be described by a solution of the macroscopic diffusion equation with a diffusion coefficient D' and a mean life time τ' in the excited state. The motion in the excited state is in general so rapid that τ' will be small compared with $\tau_j - \tau'$, the mean life time of the trapped state. From a combination of the probability that a spin will be at $\boldsymbol{r}$ in $d\boldsymbol{r}$ relative to the site it has vacated at $t = 0$ and the probability that the spin becomes trapped again after time t, one can obtain the probability $P(\boldsymbol{r})d\boldsymbol{r}$ that a single jump, or a single life in the excited state, will find the spin at $\boldsymbol{r}$ in $d\boldsymbol{r}$ from its starting place, in the same form as the macroscopic diffusion

$$P(\boldsymbol{r}) = \frac{1}{4\pi D'\tau' r} \exp\left(-\frac{r}{\sqrt{D'\tau'}}\right). \qquad (1)$$

At this stage D' is related to the overall diffusion coefficient D as

$$D'\tau' = \frac{1}{6}\langle r^2\rangle = D\tau_j, \tag{2}$$

where $\langle r^2\rangle$ is a mean squared flight distance in the time interval τ_j. If the mean life time τ' in the thermally activated state is considerably short, the mean time τ_j between two jumps corresponds to a life time of the trapped state. Equation (2) means that in the time interval τ' a diffusing spin on average jumps by a distance $\sqrt{\langle r^2\rangle}$ which is equal to that in the overall macroscopic flight. Adopting Eqs. (1) and (2) for the thermally activated diffusion, Torrey has derived a correlation function of the dipolar interaction between the two spins.

Using this correlation function, Krüger (1969) has obtained a correlation time τ_c of the diffusing spin in the thermally activated diffusion process in the form

$$\tau_c = \tau_j + \frac{a^2}{5D} = \left(1 + \frac{12a^2}{5\langle r^2\rangle}\right)\tau_j, \tag{3}$$

where a is the closest distance of the interacting two spins. Since in our case the paramagnetic ions are fixed in space, τ_j is twice as large as τ_j in Krüger's equation. In the present case considered, τ_c is a correlation time of the randomly fluctuating magnetic field in the electron-nuclear dipolar interaction. In Eq. (3), τ_c is composed of two terms. The second term in the right hand side makes the mean life time τ_j long to a certain degree according to a ratio $a^2/\langle r^2\rangle$; thus, when a mean flight distance $\sqrt{\langle r^2\rangle}$ is smaller than the closest distance of approach, autocorrelation of the randomly fluctuating field is left alive and τ_c becomes long.

By use of this model of translational motion, the following formula for T_1 can be derived for the present case where $\omega_S\tau_s \gg 1$ has been assumed

$$\frac{1}{T_1} = \frac{8\pi}{15}\cdot\frac{\hbar^2\gamma_I^2\gamma_S^2 N_S}{a^3\omega_I}S(S+1)\cdot f(\alpha, y). \tag{4}$$

The function $f(\alpha, y)$ is defined as

$$\begin{aligned} f(\alpha, y) = 3\left(\frac{1}{5}+\alpha\right)\frac{1}{y}\Bigg[& v\left(1 - \frac{1}{u^2+v^2}\right) \\ & + \left\{2 + v\left(1 + \frac{1}{u^2+v^2}\right)\right\}e^{-2v}\cos 2u \\ & + u\left(1 - \frac{1}{u^2+v^2}\right)e^{-2v}\sin 2u\Bigg] \end{aligned} \tag{5}$$

with

$$\left.\begin{matrix} u \\ v \end{matrix}\right\} = \frac{1}{2}\sqrt{\frac{q(1\pm q)}{\alpha}}, \tag{6}$$

$$\frac{1}{q} = \sqrt{1 + \frac{1}{y^2}\left(1 + \frac{1}{5\alpha}\right)^2}, \tag{7}$$

$$y = \omega_I\tau_c, \tag{8}$$

$$\alpha = \frac{\langle r^2\rangle}{12a^2}. \tag{9}$$

Here, S, N_S and ω_S are the electron spin, the concentration and the Larmor frequency of the Fe^{3+} ion, respectively, and ω_I is the Larmor frequency of the nuclear spin observed.

4. Results and Discussion

4.1. Adsorption Isotherms and Adsorption Heat of the CHF_3 Molecule

For understanding CHF_3 adsorption phenomena on the NaY5.6 zeolite from the volumetric viewpoint, adsorption amounts at various equilibrium pressures P were measured at 273 and 293 K. The adsorption isotherms obtained are shown in Fig. 1, where the ordinate is a number n of the adsorbed CHF_3 molecules per unit cell; 1 unit cell $Na_{50}(AlO_2)_{50}(SiO_2)_{142}$ as a dried zeolite. The solid lines in Fig. 1 are the result calculated from Hill's equation (Hill, 1946, 1947). This equation is given as

$$P = \frac{\theta}{K_1(1-\theta)}\exp\left(\frac{\theta}{1-\theta} - K_2\theta\right), \tag{10}$$

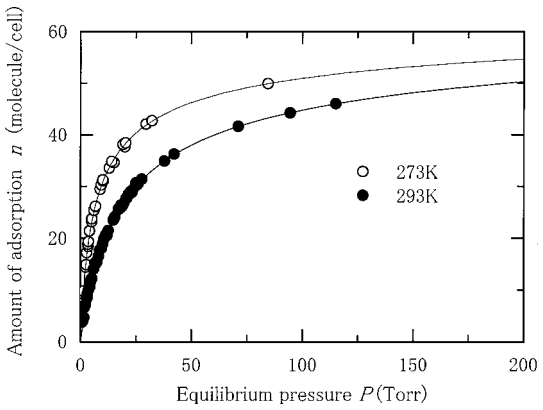

Figure 1. Adsorption isotherms of the CHF_3 molecule on NaY5.6 zeolite at 273 and 293 K. The curves are the result obtained from the least square fit of the experimental data to Hill's equation.

Table 2. Adsorption parameters of the CHF_3 on NaY5.6 zeolite fitted to Hill's equation.

Temperature (K)	K_1	K_2	V_m	Data point
273	0.1234	0.0684	77.60	29
293	0.0409	0.1920	79.92	59

where P is the equilibrium pressure, θ the surface coverage, K_1 the equilibrium constant of adsorbate-adsorbent (Henry constant), and K_2 that of adsorbate-adsorbate. In Eq. (10), the coverage θ is given by a volume ratio V/V_m, where V is a CHF_3 gas volume under standard conditions (273 K, 1 atm) corresponding to an adsorption amount at the equilibrium pressure, and V_m is its saturated value at a constant experimental temperature. The result of simulations is shown in Table 2.

The maximum adsorption amount n estimated from Hill's equation, was about 80 molecule/cell. This number corresponds to 10 CHF_3 molecules in a supergage which has 4 Na cations on its surface.

In both adsorption isotherms, we can see change in the inclination of isotherms around $n \simeq 30$–40 molecule/cell. Namely, a number n of adsorbed molecules increases linearly with an equilibrium pressure up to this amount $n \approx 30$ molecule/cell and then begins to saturate. As regards location of the charge compensating Na^+ in the Y zeolite, it is well known that there are 16 cation sites, Site I, per unit cell in the center of hexagonal prisms and 32 sites, Site II, on the surface of supergages (Sherry, 1968; Mortier, 1984). The CHF_3 molecule is not accessible to a Site I. From a close correspondence between the change in inclination of isotherms around $n \simeq 30$–40 molecule/cell and the number of Na^+ at Site II it should be noted that the Na cation on a surface is an adsorption site for the CHF_3.

Figure 2 shows an isosteric differential heat of adsorption obtained from the adsorption isotherms, by use of Clapeyron-Clausius equation, together with the condensation heat of about 17 kJ/mol which was estimated from the temperature dependence of a saturation pressure reported by Asahi Glass Co. In Fig. 2 the adsorption heat decreases gradually with increasing an adsorption amount.; it is about 35 kJ/mol up to $n \simeq 10$ molecule/cell and reduces to 23 kJ/mol at $n \simeq 55$ molecule/cell. As compared with the adsorption heat of a $CHClF_2$ molecule adsorbed on the same NaY zeolite, which is about 50 kJ/mol up to $n \simeq 30$ molecule/cell (Yoshikawa et al., 2000), physical adsorption of CHF_3 is weaker than that of $CHClF_2$.

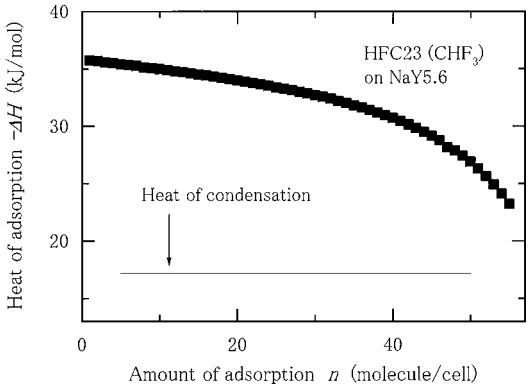

Figure 2. Adsorption amount dependence of the isosteric differential heat of adsorption $-\Delta H$ for the CHF_3 molecule on NaY5.6 zeolite and the heat of condensation for CHF_3.

4.2. Chemical Shifts of H and F NMR Spectra

H and F NMR spectra of a CHF_3 molecule adsorbed on the NaY zeolite were measured for adsorption amounts over a range of $n = 6.5$–55 molecule/cell. Every spectra of H measured at 400 MHz and F at 376 MHz had a nearly single Lorentian line shape and the full halfwidth of 200 to 250 Hz. In general, change in the electronic environment of a nuclear spin results in a shift of its resonance frequency based on variation in screening of the static magnetic field. Figures 3(a) and (b) show dependences on n of a chemical shift for H and F, respectively. At the smallest value of $n = 4.5$ molecule/cell in Fig. 3(a), the chemical shift of H is the largest with respect to TMS, which corresponds to the finest screening (Pople et al., 1959). On the other hand, the F chemical shift at the same n in Fig. 3(b) is the lowest with respect to $CFCl_3$, which means the largest electronic shielding of a F nucleus. The chemical shift of H decreases linearly with increasing n, while the one of F increases with the same increase in n. Namely, an increase in n produces more effective shielding of the H nucleus and less one of F. These changes in the chemical shifts indicate that the electron distribution in the CHF_3 molecule shifts to the side of F atoms in the lowest range of n, and that the increase in n will get the concentrated electrons free from the F atoms.

The surface of a zeolite supergage is made up mainly of negatively charged oxygen atoms and positively charged Na atoms. Since the polar CHF_3 molecule has excess negative charges around the F atoms in an unadsorbed state, these negative charges can be more stabilized in a potential of the Na^+ cation. Therefore, in the

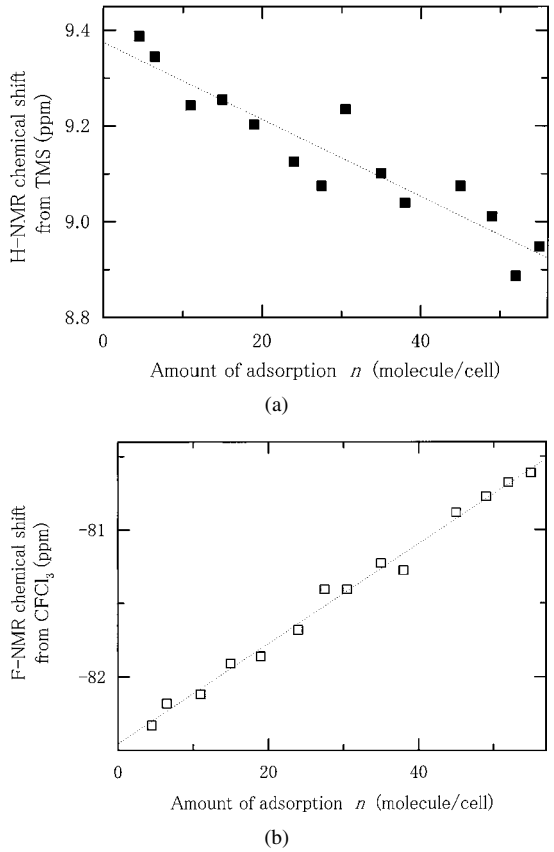

Figure 3. Adsorption amount dependence of the NMR chemical shift of the CHF_3 molecule adsorbed on NaY5.6 zeolite at room temperature. (a) H NMR. The chemical shift is referred to TMS. (b) F NMR. The chemical shift is referred to $CFCl_3$. Dotted lines are linearly fitted by the method of least squares.

adsorbed state, the F atoms are located near the Na atom and the H is far from it. As shown in Fig. 4, therefore, we can conclude that the Na atom comes nearly into a line of the molecular symmetry axis connecting C and H atoms. This adsorption structure of CHF_3 is the same as that in the case of $CHClF_2$ (Yoshikawa et al., 2000). When n is increased, the adsorbed molecules are destabilized by mutual molecular collisions and a lifetime of the adsorbed state is shortened. Thus the observed resonance frequency approaches, on an average, to the one in the state free from the potential of the Na^+ cation with the increase in the adsorption amount.

4.3. Temperature Dependence of T_1 and Relaxation Analysis by Translational Diffusion

For H and F nuclei in the CHF_3 molecule adsorbed on the zeolite, temperature dependences of T_1 are shown

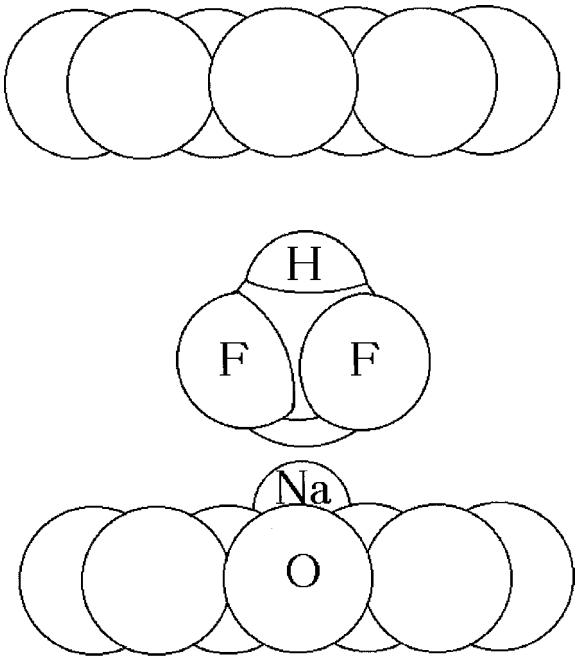

Figure 4. Adsorptive coordination model of the CHF_3 molecule on the Na^+ site in the wall surface of NaY5.6 zeolite.

in Figs. 5 and 6, respectively, at the three representative adsorption amounts n. At first sight one finds that T_1 of F is 2 or 3 times as long as T_1 of H over the temperature range observed. As will be shown shortly in this section, this T_1 ratio of H and F may reflect a difference in the closest distance of approach to the relaxing partner spin, namely, a Fe^{3+} electron spin in the case considered here.

Both Figs. 5 and 6 contain T_1 data at the two frequencies, and they show that T_1 considerably depends on the observation frequency. At the high frequency around 400 MHz, T_1 definitely has a minimum in the temperature range observed and the T_1 minimum shifts toward low temperatures with increasing n. Roughly speaking by assuming a single correlation time τ_c of the adsorbed molecule, this trend is explained by a decrease in τ_c with increasing n. However, there is a distinction between H and F in the n dependence of a T_1 minimum value, $T_{1\,\mathrm{min}}$. While $T_{1\,\mathrm{min}}$ of H does not substantially depend on n, the one of F becomes short with increasing n. These features in our result are in a marked contrast with those in the work by the Leipzig group for cyclohexane adsorbed on a commercial NaY zeolite (Pfeifer, 1976b; Pfeifer et al., 1979). From H relaxation measurements for cyclohexane at 16 MHz, Pfeifer and his collaborators showed that the $T_{1\,\mathrm{min}}$

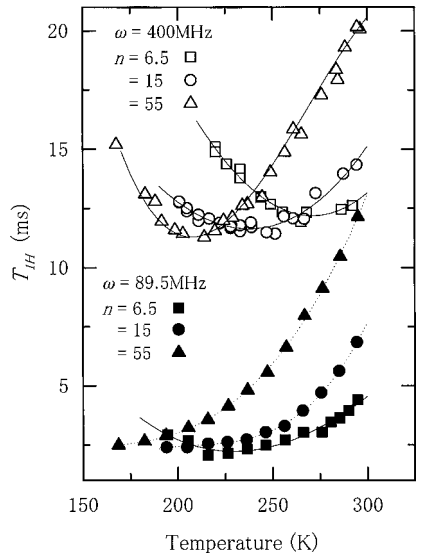

Figure 5. Temperature dependences of the longitudinal relaxation times measured at 89.5 and 400 MHz for a H nucleus in the CHF_3 molecule adsorbed on NaY5.6 zeolite with the loading amounts of $n = 6.5, 15$ and 55 mole/cell. The dotted and solid lines are calculated on the basis of the diffusion model.

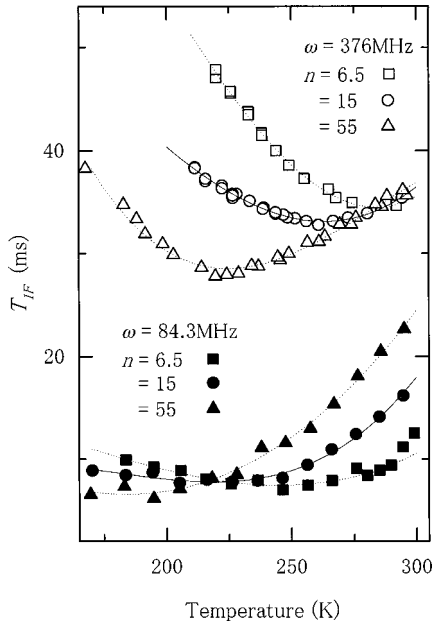

Figure 6. Temperature dependences of the longitudinal relaxation times measured at 84.3 and 376 MHz for a F nucleus in the CHF_3 molecule adsorbed on NaY5.6 zeolite with the loading amounts of $n = 6.5, 15$ and 55 mole/cell. The dotted and solid lines are calculated on the basis of the diffusion model.

occurred at the same temperature and had the same value over a wide pore filling factor $\theta = 0.2$–0.9, whereas its shape became flatter with increasing θ. The same features are found in H relaxations measured at 30 MHz for various n-paraffins adsorbed on a NaX zeolite (Kärger et al., 1980).

As for the low frequency data around 90 MHz, every T_1 data for the three n's are several times as short as each corresponding one at the high frequency. By use of a Lorentzian spectral density with a correlation time τ_c (Abragam, 1961), these short T_1 values at the low frequency can qualitatively be interpreted on the basis of a breakdown of the extremely narrowing condition, namely, $\omega\tau_c \ll 1$; thus, molecular motion of the CHF_3 in the zeolite is not so rapid as in an isotropic liquid or gas. If τ_c becomes long with decreasing temperature, the thermal motion is more effective in the low frequency than in the high frequency, as can be seen at $T \sim 200$ K in Figs. 5 and 6. Based on these conjectures, we at first tried to analyze all the T_1 data phenomenologically by assuming the Lorentzian spectral density. But it failed because of the large difference of changes in T_1 at the two frequencies. For a quantitative analyses, therefore, we adopt the translational diffusion model described in the previous chapter.

We have measured longitudinal relaxations for the two nuclear spins H and F in the same CHF_3 molecule. Since a molecule jumps as a whole from one trapping site to another in the translational diffusion process, the mean jump time τ_j and the mean squared jump distance $\langle r^2 \rangle$ are common to the relaxation of the two spins. On the other hand, the closest distance of approach, a, between a Fe^{3+} ion and a nucleus observed can be set as a different variable for each nucleus, because it has a sensitive effect on the dipolar relaxation. In the relaxation analysis of our T_1 data, therefore, we set four independent parameters τ_j, $\langle r^2 \rangle$, a_H and a_F. By using values of these parameters assumed and an concentration N_S of the Fe^{3+} estimated from the X-ray emission data, T_1 values of H and F at the respective two frequencies were calculated from Eqs. (4) to (9) for each experimental temperature. Best fitted results obtained by the least square method are shown by solid or dotted lines in Figs. 5 and 6. The agreement between the experimental results and the calculated values is satisfactory for every T_1 data. In Figs. 7 to 11, values of the various parameters thus determined are plotted as a function of temperature T.

Figure 7 shows the closest distance of approach a_H and a_F to a Fe^{3+} ion for H and F nuclei, respectively.

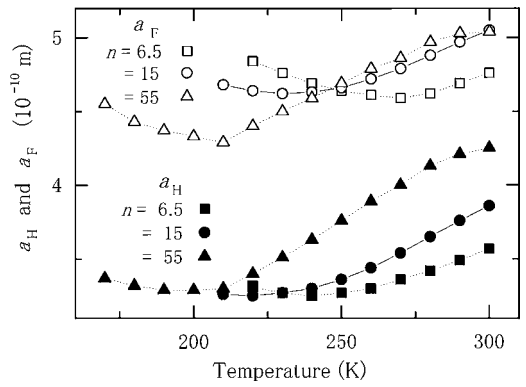

Figure 7. Temperature dependences of the closest distances of approach, a_H and a_F, between a paramagnetic impurity and measured nuclei H and F, respectively, for the loading amounts of $n = 6.5$, 15 and 55 mole/cell. The dotted and solid lines are added only to guide the eye.

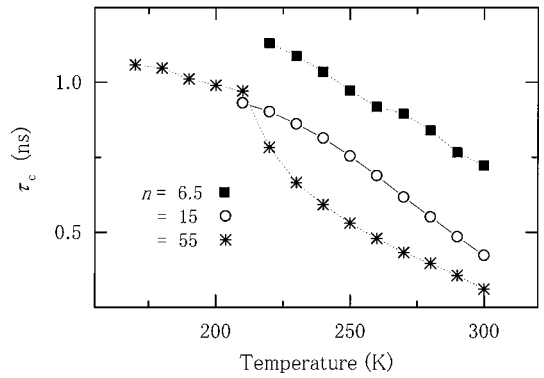

Figure 8. Temperature dependences of the correlation time τ_c of the dipolar field for the loading amounts of $n = 6.5$, 15 and 55 mole/cell. The dotted and solid lines are added only to guide the eye.

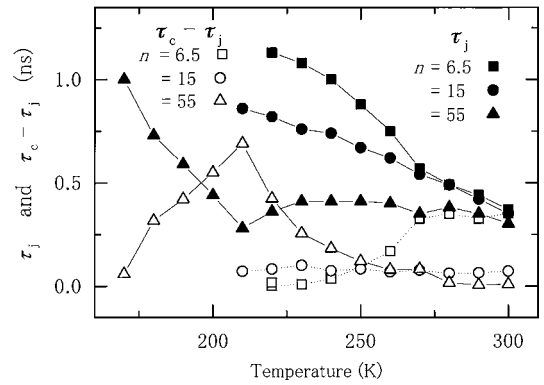

Figure 9. Temperature dependence of the adsorption life time τ_j and the difference $\tau_c - \tau_j$ for the loading amounts of $n = 6.5$, 15 and 55 mole/cell. The definition of τ_j is given in the text. The dotted and solid lines are added only to guide the eye.

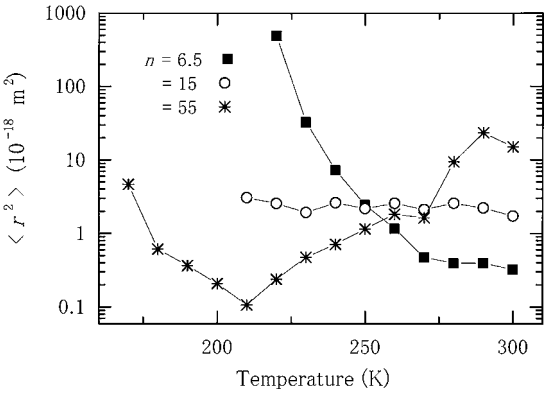

Figure 10. Temperature dependences of the mean squared jump distance $\langle r^2 \rangle$ in the diffusion of the CHF_3 molecules for the loading amounts of $n = 6.5$, 15 and 55 mole/cell. The solid lines are added only to guide the eye.

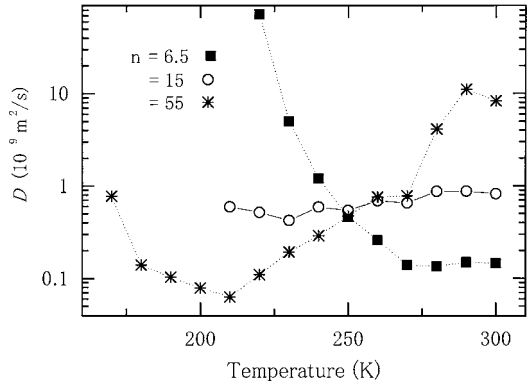

Figure 11. Temperature dependences of the diffusion coefficient D of the adsorbed CHF_3 molecules for the loading amounts of $n = 6.5$, 15 and 55 mole/cell. The dotted and solid lines are added only to guide the eye.

For all of the three cases of n, a ratio a_F/a_H is 1.2 to 1.4 over the temperature range observed. Since T_1 is proportional to $1/a^6$, an appreciable part of the difference in T_1 between H and F can be explained by this ratio. A conspicuous feature seen in Fig. 7 is an increase in a_H and a_F with T for $n = 55$ molecule/cell in the high temperature region of $T = 210$–300 K. As will be shown shortly, this increase reflects a liquid-like behavior of the adsorbate. In the high loading case ($\theta \simeq 0.7$) of $n = 55$ molecule/cell, adsorption of a CHF_3 molecule is weak and the heat of adsorption is only 23 kJ/mol. Increases in a mobility of the adsorbate liquid as well as in mutual collision of the CHF_3 molecules result in the increase in a_H and a_F with T. Since adsorption for $n = 6.5$ molecule/cell is strong as

compared with that for $n = 55$ molecule/cell, a_H and a_F are shorter than those for $n = 55$ molecule/cell in the same high temperature range of $T = 260$–300 K. On the other hand, a little unfamiliar effect is observed in low temperatures both for $n = 55$ molecule/cell and 6.5 molecule/cell. In this temperature range, a_F especially increases with decreasing T. This may be attributed to steric hindrance in the zeolite lattice. Since a F atom is more bulky than H, this effect is rather outstanding for F. A Fe^{3+} ion is substitutionally at an Al^{3+} site and is coordinated tetrahedrally by four O^{2-} ions. When thermal vibration of the zeolite becomes weak, then, the steric hindrance becomes large in low temperatures. In the low temperature range, furthermore, a_F for $n = 55$ molecule/cell is considerably shorter than for $n = 6.5$ molecule/cell; this short distance is possibly brought about by lattice distortion due to the high loading at $n = 55$ molecule/cell.

As for the correlation time τ_c shown in Fig. 8, τ_c decreases monotonically from about 1ns to 0.4 ns with increasing T for all cases of n. At a same temperature, τ_c for the case of $n = 6.5$ molecule/cell with a large heat of adsorption is the longest among the three cases. Since τ_c consists of two terms, it is necessary to consider an effect of individual term separately. Then, next let us consider temperature dependences of τ_j and $\langle r^2 \rangle$ for $n = 6.5$ molecule/cell and $n = 55$ molecule/cell as two extreme cases of low and high loadings. Temperature dependences of τ_j and $\langle r^2 \rangle$ are shown in Figs. 9 and 10, respectively, for the three cases of n. Figure 9 also contains plotting of a difference $\tau_c - \tau_j$.

In the case of the low loading ($n = 6.5$ molecule/cell), the life time τ_j of the trapped state as well as the jump distance $\sqrt{\langle r^2 \rangle}$ decrease monotonically from 1.1 ns to 0.4 ns and from 220 Å to 5.7 Å, respectively, with increasing T over the whole range of $T = 220$–300 K. An activation energy of τ_j is equal to 8.1 kJ/mol. These decreases are attributed to destabilization of the trapped state due to activated thermal vibration and frequent mutual collision between the short-lived CHF_3 molecules. As for the case of $n = 55$ molecule/cell in the low temperature range of $T = 170$–210 K, one can find the same degree of decreases in τ_j and $\sqrt{\langle r^2 \rangle}$ as those for $n = 6.5$. An activation energy of this τ_j is 8.9 kJ/mol which is nearly equal to the one for $n = 6.5$ molecule/cell. Thus, these decreases are due to the same origin with the case of $n = 6.5$ molecule/cell. In the high temperature range of $T = 210$–300 K for $n = 55$ molecule/cell, however, τ_j is about 0.4 ns and is insensible to temperature over the whole temperature range; an activation energy of τ_j is so small as 1.2 kJ/mol. On the other hand, the jump distance $\sqrt{\langle r^2 \rangle}$ increases rapidly with T from about 3 Å at $T = 210$ K to 48 Å at $T = 290$ K. These results may be explained by the assumption that the adsorbate of CHF_3 molecules as a whole are flowing about in a liquid-like state in the high temperature range. Thus, a state of the adsorbate changes from an adsorbed gas state to liquid-like one at the temperature of $T = 210$ K.

Temperature dependences of the diffusion coefficient D for the three values of n are shown in Fig. 11, which are obtained from Figs. 9 and 10 by use of the equation $\langle r^2 \rangle = 6\, D\tau_j$. One of the most conspicuous features in this figure is the relatively large magnitude of D and the negative value of a derivative, $dD/dT < 0$, for $n = 6.5$ and 55 molecule/cell. These are characteristic of the CHF_3 molecule adsorbed on the NaY zeolite. We have also done similar T_1 measurements for a $CHClF_2$ molecule adsorbed on the same NaY zeolite, detailed analysis of which will be reported in a forthcoming paper. As for the $CHClF_2$ molecule at $\theta = 0.8$, the diffusion coefficient increases monotonically with temperature over a whole range of $T = 180$–300 K, but it is an order of magnitude smaller than that of the CHF_3 molecule adsorbed at the loading $\theta = 0.7$ ($n = 55$ molecule/cell); for example, they are $D = 1.05 \times 10^{-10}$ m^2/s at 250 K and 2.03×10^{-10} m^2/s at 300 K. These values for $CHClF_2$ at $\theta = 0.8$ on NaY5.6 are fairly similar to the values for $CHClF_2$ ($n \simeq 40$ molecule/cell) on a NaX zeolite which are directly obtained by the pulse gradient NMR method (Kärger et al., 1988). It is known that mobility of benzene molecules adsorbed on NaX is higher than the one adsorbed in NaY and this difference of D values is attributed to the interaction between benzene molecule and the nonlocalizable Na^+ on NaX (Pfeifer, 1976b). Thus the coinciding diffusivities of $CHClF_2$ molecules in both NaX and NaY show that there is no contribution from the interaction with the nonlocalizable Na^+ for $CHClF_2$ and our method of T_1 analysis is reliable.

Since τ_j in Fig. 9 changes at most by a factor of 2–3 over the whole temperature range of $T = 180$–300 K, the temperature dependences of D are mainly attributed to the large changes in $\langle r^2 \rangle$ by a factor of 10–100 over the same temperature range. The coefficient D for $n = 55$ molecule/cell increases rapidly with T from 6×10^{-11} m^2/s at $T = 210$ K to 6×10^{-9} m^2/s at $T = 290$ K. The usual Arrhenius plot is thought to hold for this temperature dependence. An activation energy of D is equal to 29.9 kJ/mol. This large value

of D in the high temperature range reflects fluidity of the CHF_3 molecule in the liquid-like state.

On the other hand, there is no such flow of the molecules as a whole in both cases of $n = 6.5$ molecule/cell and of $n = 55$ molecule/cell at low temperatures, because of a small number of untrapped molecules in a supercage for $n = 6.5$ molecule/cell and low thermal energy of the molecules for $n = 55$ molecule/cell at low temperatures. Thus, collisions of the molecule with a surrounding zeolite lattice for $n = 6.5$ molecule/cell and mutual collisions between the molecules for $n = 55$ molecule/cell take place more frequently as the temperature rises. These collisions result in the decrease in $\langle r^2 \rangle$; thus the large shortening of a mean jump distance $\sqrt{\langle r^2 \rangle}$ with increasing T gives rise to the negative value of dD/dT. These behaviors characteristic of the CHF_3 molecule are also related with slightly weak interaction with Na^+ at Site II, namely, the low heat of adsorption of this molecule and they are in line with the fact that the CHF_3 gas has a high value of saturated vapor pressure as well as high mobility based on a symmetry of the molecule as compared with the $CHClF_2$ gas.

As for the case of $n = 15$ molecule/cell, temperature dependences of the parameters τ_c, τ_j, $\langle r^2 \rangle$ and D show a feature intermediate between the cases of $n = 6.5$ molecule/cell and $n = 55$ molecule/cell.

At last, we remark on the gradually monotonous decrease in τ_c with increasing T. This simple change in τ_c is due to the effect of the second term in Eq. (3). Because of this term, the life time τ_j of the trapped state is effectively multiplied by a factor of $1 + 12a^2/5\langle r^2 \rangle$, as discussed in the previous chapter. Since $\langle r^2 \rangle = 6\,D\tau_j$, a decrease in τ_j with increasing T can be in some degree counterbalanced by this factor when D and/or τ_j decrease with T. As clearly seen in Fig. 9, this effect can be found for the cases of $n = 6.5$ molecule/cell in the high temperature range of $T = 270$–300 K, and of $n = 55$ molecule/cell in the transition temperature range of $T = 180$–220 K.

4.4. Adsorption Amount Dependence of T_1

Relationships between an adsorption amount n and T_1 observed at about 90 MHz are shown Fig. 12 for H and F nuclei; the experimental temperature is kept at 273 K and n ranges from 4.5 molecule/cell to 55 molecule/cell. As can be seen in Fig. 12, T_1 increases linearly with n in the low loading region of $n \leq 25$. In the intermediate region of $n = 25$–40 molecule/cell,

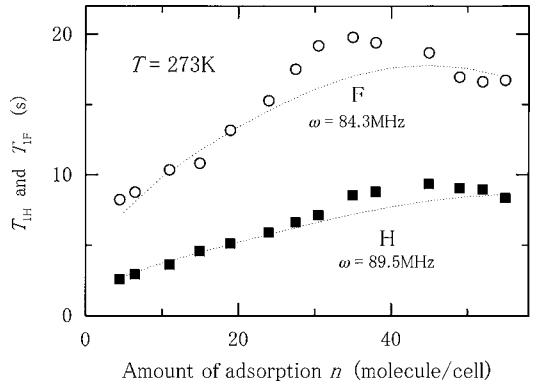

Figure 12. Adsorption amounts dependences of the longitudinal relaxation times for H and F nuclei in the CHF_3 molecule at 273 K. The dotted curves are calculated by use of adsorption amount dependences of the four parameter a_H, a_F, τ_j and $\langle r^2 \rangle$ at 273 K.

the increase in T_1 saturates and attains to a maximam value. Further increase in n gives rise to decreasing T_1 in the high loading region.

These changes in T_1 with respect to n have been analyzed by use of the results obtained in the previous section. At first, from temperature dependences of the four parameters a_H, a_F, τ_j and $\langle r^2 \rangle$ shown by solid or dotted lines in Figs. 7, 9 and 10, we obtained values of the four parameters at $T = 273$ K for the three cases of $n = 6.5$, 15 and 55 molecule/cell, and expressed each of the four parameters by a quadratic function of n. Using these relations and Eqs. (4) to (9), we next calculated T_1 values for H and F as a function of n, the result of which were shown by dotted lines in Fig. 12. Around $n = 6.5$, 15 and 55 molecule/cell, calculated values of T_1 are in good agreement with experimental ones within experimental errors. Discrepancies between experimental and calculated values in the intermediate loading of $n = 30$–40 molecule/cell are due to lack of experimental T_1 data at the high frequency around 400 MHz. As can be seen in Figs. 7 and 10, values of a_F and $\langle r^2 \rangle$ at $n = 15$ molecule/cell are near to the ones at $n = 55$ molecule/cell as compared with those to the ones at $n = 6.5$ molecule/cell. Consequently, the parameters especially for F which are estimated from the quadratic functions have fairly large values in this intermediate region of n.

The experimental changes in T_1 with increasing n can be explained in terms of variations in the parameters a_H, a_F, τ_j and $\langle r^2 \rangle$. In the low loading region at $T = 273$ K, the increases in a_H, a_F and $\langle r^2 \rangle$ with increasing n together with the decrease in τ_j result in the increase in T_1, as seen in Fig. 12. In the high loading

region of $n > 40$–50 molecule/cell, the adsorbate at 273 K is in the liquid-like state with a rather high mobility. The lifetime τ_j still keeps on decreasing with increasing n and this change has an effect to make T_1 long. On the other hand, a_H and especially a_F as well as $\langle r^2 \rangle$ decrease with increasing n in this high loading region. Since all of these changes make T_1 short, their effects counterbalance and rather overcome the effect of τ_j

5. Conclusion

1. Fairly short relaxation times T_1 such as several ms to a few tens ms for H and F nuclei in a molecule adsorbed on a NaY zeolite, result from the nuclear-electron dipolar interaction with a Fe^{3+} ion contained in the commercial zeolite.
2. Several different experimental relationships of T_1 with an adsorption amount n, temperature T and an observation Larmor frequency ω were fairly well reproduced from calculations based on the translational diffusion of the adsorbed molecule.
3. By adopting the thermally activated diffusion model proposed by Torrey, temperature and loading dependences of various parameters which determine microdynamic behaviours in the small pores of the zeolite can be estimated from the analysis of T_1 relaxation data.
4. In the low loading case of $n \leq 10$–15 molecule/cell as well as in low temperatures even for a high loading case, microdynamics of the CHF_3 molecules in the NaY5.6 zeolite is dominated by thermal activation of the trapped state and resultant increase in mutual collision between the CHF_3 molecules. In the high loading case of $n \geq 40$–50 molecule/cell, the CHF_3 molecules as a whole behave liquid-like in high temperatures. At $n = 55$ molecule/cell, a transition to this liquid-like state with increasing T was clearly found out in the change of $\langle r^2 \rangle$ obtained from the relaxation analysis.

Nomenclature

a_F	Closest distance of approach between a F nucleus and a Fe^{3+} ion
a_H	Closest distance of approach between a H nucleus and a Fe^{3+} ion
D	Diffusion coefficient of an adsorbate molecule
D'	Diffusion coefficient in the thermally activated state
γ_I	Gyromagnetic ratio of a measured nucleus I
γ_S	Gyromagnetic ratio of an electron spin in the Fe^{3+} ion
$\hbar$	Dirac constant
ΔH	Enthalpy change on adsorption
n	Number of the adsorbed CHF_3 molecule per unitcell in the zeolite
N_S	Number of a Fe^{3+} ion per cm^3
P	Equilibrium pressure
$P(r)$	Distribution probability of a nuclear spin at $\boldsymbol{r}$
$\langle r^2 \rangle$	Mean squared jump distance in diffusion
S	Electron spin quantum number of a Fe^{3+} ion
θ	Coverage
T	Temperature
T_1	Longitudinal relaxation time
T_{1F}	Longitudinal relaxation time for a F nucleus
T_{1H}	Longitudinal relaxation time for a H nucleus
$T_{1\,\min}$	Minimum of a longitudinal relaxation time
τ'	Life time of the thermally activated state
τ_c	Correlation time of the magnetic dipolar field
τ_j	Mean jump time or adsorption life time
ω	Larmor frequency
ω_I	Larmor frequency of a measured nucleus I
ω_S	Larmor frequency of an electron spin in the Fe^{3+} ion

References

Abragam, A., *Principles of Nuclear Magnetism*, Chap. 8, Clarendon, Oxford, 1961.

Derouane, E.G., M. Mestdagh, and L. Vielvoye, "EPR Study of the Nature and Removal of Iron(III) Inpurities in Ammonium-Exhanged NaY-Zeolite," *J. Catal.*, **33**, 169–175 (1974).

Fraissard, J., *Physical Adsorption: Experiment, Theory and Applications*, Kluwer Academic Publishers, 1997.

Hill, T.L., "Statistical Mechanics of Multimolecular Adsorption II. Localized and Mobile Adsorption and Absorption," *J. Chem. Phys.*, **14**, 441–453 (1946).

Hill, T.L., "Statistical Mechanics of Multimolecular Adsorption. III. Introductory Treatment of Horizontal Interactions. Condensation and Hysteresis," *J. Chem. Phys.*, **15**, 767–777 (1947).

Ishiwata, M. and T. Ono, "Probe Dynamics of Chloroform in a Smectic Liquid Crystal. I. ^{13}C and ^{1}H NMR Relaxation," *J. Phys. Soc. Jpn.*, **64**, 636–642 (1995).

Kärger, J. and D.M. Ruthven, *Diffusion in Zeolites and other Microporous Solids*, John Wiley & Sons, New York, 1992.

Kärger, J., H. Pfeifer, M. Rauscher, and A. Walter, "Self-diffusion of *n*-Paraffins in NaX Zeolite," *J.C.S. Faraday I*, **76**, 717–737 (1980).

Kärger, J., H. Pfeifer, S. Rudtsch, and W. Heink, "^{19}F NMR Diffusion Study of Molecules Adsorbed on Zeolites," *J. Fluorine Chem.*, **39**, 349–356 (1988).

Krüger, G.J., "Magnetische Relaxation durch Translations Diffusion in Flüssigkeiten," *Z. Naturforsch.*, **24a**, 560–565 (1969).

Michel, V.D. and J. Thöring, "Kernspin Relaxation zum Studium des Adsorptionsverhaltens von Cyclohexan an NaY-Zeolithen," *Z. Phys. Chemie*, Leipzig, **247**, 85–90 (1971).

Mortier, W.J., E. Van den Bossche, and J.B. Uytterhoeven, "Influence of the Temperature and Water Adsorption on the Cation Location in Na-Y Zeolites," *Zeolites*, **4**, 41–44 (1984).

Pfeifer, H., "Surface Phenomena Investigated by Nuclear Magnetic Resonance," *Phys. Rep.*, **26C**, 293–340 (1976a).

Pfeifer, H., "Adsorption Phenomena in Zeolites as Studied by Nuclear Magnetic Resonance," *Coll. and Interface Sci. ACS Symposium Ser.*, **34**, 36–47 (1976b).

Pfeifer, H. and H. Winkler, "The Microdynamic Behaviour of Simple Hydrocarbons Adsorbed in Porous Solids," in *Proc. 4th Spec. Coll. Ampere*, Leipzig, 31–40 (1979).

Pople, J.A., W.G. Schneider, and H.J. Berstein, *High-Resolution Nuclear Magnetic Resonance*, Ch. 7, McGraw-Hill, New York, 1959.

Resing, H.A. and J.K. Thompson, "NMR Relaxation in Adsorbed Molecules. V. SF_6 on Faujasite: Dipolar Coupling of Fluorine Nuclei to Ferric-Ion Impurities," *J. Chem. Phys.*, **46**, 2876–2880 (1967).

Rudziński, W., W.A. Steele, and G. Zgrabich, *Equilibria and Dynamics of Gas Adsorption on Heterogeneous Solid Surfaces*, Elsvier Science B.V., 1997.

Sherry, H.S., "The Ion-Exchange Properties of Zeolites. IV. Alkaline Earth Ion Exchange in the Synthetic Zeolites Linde X and Y," *J. Phys. Chem.*, **72**, 4086–4094 (1968).

Torrey, H.C., "Nuclear Spin Relaxation by Translational Diffusion," *Phys. Rev.*, **92**, 962–969 (1953).

Werbelow, L.G. and D.M. Grant, "Intramolecular Dipolar Relaxation in Multispin Systems," *Adv. Mag. Reson.*, **9**, 189–299 (1977).

Yoshikawa, M., T. Yoshida, M. Ishiwata, T. Hasegawa, and S. Ozawa, "The Adsorption of $CHClF_2$ on NaY5.6 Zeolite," *Adsorption*, **3**, 259–267 (2000).